Measurement of the human respiratory tract deposited surface area of particles with an electrical low pressure impactor

Teemu Lepistö[a], Heino Kuuluvainen[a], Paxton Juuti[a], Anssi Järvinen[a], Anssi Arffman[b] and Topi Rönkkö[a*]

[a]*Aerosol Physics Laboratory, Faculty of Engineering and Natural Sciences, Tampere University, Tampere, Finland;*

[b]*Dekati Ltd., Tampere, Finland;*

Corresponding author:

Topi Rönkkö

Aerosol Physics Laboratory

Faculty of Engineering and Natural Sciences

Tampere University

Streed address: Korkeakoulunkatu 3, 33720, Tampere, Finland

Postal address: P.O.Box 692, 33014 Tampere, Finland

Email: topi.ronkko@tuni.fi

Measurement of the human respiratory tract deposited surface area of particles with an electrical low pressure impactor

Particle deposition in the human respiratory tract is considered to have negative effects on human health. The lung deposited surface area (LDSA) is an important metric developed to assess the negative health effects of particles deposited in the alveolar region of the human respiratory tract. The measurement of the LDSA is frequently based on the detection of the electrical current carried by diffusion charged particles. Various conversion factors can be used to convert the electric current into LDSA concentration with relatively good accuracy up to the size about 300-600 nm. In this study, we introduce stage-specific LDSA conversion factors for electrical low pressure impactor (ELPI+) data, which enable accurate and real time LDSA concentration and LDSA size distribution measurements in the particle size range from 6 nm to 10 µm. This wide size range covers most of the alveolar deposition of particles, which has not been possible previously by electrical methods. Also, the conversion factors for tracheobronchial and head airways particle surface area deposition were determined, and the stage-specific conversion factors were compared with the single-factor data conversion method. Furthermore, the stage-specific calibration was tested against real-world particle size distributions by simulations and against laboratory-generated aerosols. Particles larger than 300 nm were observed to significantly affect the total LDSA concentration. Stage-specific conversion factors are especially required while measuring aerosols containing larger particles or when considering the surface area deposition in the tracheobronchial region and head airways. The method and the conversion factors introduced in this study can be used to monitor LDSA concentrations reliably in various environments containing particles in different size ranges.

Keywords: human respiratory system; electrical low pressure impactor (ELPI); lung deposited surface area (LDSA); diffusion charging; surface area; particulate matter (PM);

Introduction

Particulate matter is known for causing negative health effects. Air pollution and especially fine particulate matter (PM2.5) have been strongly linked with premature deaths (i.e. Dockery et al. 1993). Today, particulate matter is still a major health problem world-wide. It has been estimated that PM2.5 causes world-wide about 3.3 million premature deaths per year (Lelieveld et al. 2015). Also, the coarse

particulate matter (PM10) has been found to affect the daily mortality rate (Meister et al. 2012). Particulate matter also contributes to the incidence of various cardiopulmonary and other diseases (Burnett et al. 2014).

The mechanisms of how particles affect human health are still unclear even though evidence for the harmful health effects of particulate matter is strong. In various toxicological studies, it has been found that the particle surface area may have a stronger correlation with the negative health effects of fine particles than the number or mass concentration (Brown et al. 2001; Oberdörster et al. 2005). A relevant metric to estimate the particle surface area concentration deposited in the alveolar region of human lungs is called the lung deposited surface area (LDSA). Especially for ultrafine particles, the LDSA is potentially the most relevant metric for the exposure since the toxicity of ultrafine particles may be higher than the toxicity of larger particles with the same composition (Johnston et al. 2000; Karlsson et al. 2009). One factor explaining this relation could be the production of harmful reactive oxygen species on particle surface, which is dependent on the reactive surface area (Hamilton et al. 2008).

The human respiratory tract can be divided into three major compartments. One of them is the above mentioned alveolar region, where the interaction between lungs and pulmonary circulation takes place. The other two main compartments are tracheobronchial region and head airways. Particle exposure in the human lungs, which consist of alveolar and tracheobronchial region, is linked to various diseases including lung cancer, acute lower respiratory tract infections and chronic obstructive pulmonary disease (Burnett et al. 2014). According to a recent study by Maher et al. (2016), fine particles pose a risk of damaging the human brains by entering directly through the olfactory nerve. This emphasizes the relevance of the head airways region in the deposition of fine particles, which may not have been considered to be relevant with respect to the negative health effects of the particulate matter, at least if compared to alveolar deposition of particles.

Majority of particles below the size of 10 µm enter the human respiratory tract and the region of deposition depends significantly on the particle

size (ICRP 1994). Larger coarse particles deposit mostly by their inertial effects, whereas nanoparticles deposit mainly by Brownian diffusion. Deposition based on the inertial effects is characterized with the aerodynamic diameter, whereas deposition by the diffusion is characterized by the mobility equivalent diameter (Hofmann 2011). To estimate particles' region of deposition accurately, both diameter concepts must be taken into account, which may cause problems in the LDSA measurements or in the calibration of instruments, because the instruments usually measure either electrical mobility or aerodynamic size, but not both. Diffusion charger based instruments are often used to measure the LDSA concentration because of the strong correlation between the LDSA concentration and the particle charge after unipolar diffusion charging in a certain particle size range. There are multiple diffusion-charger-based real-time instruments that measure LDSA, such as a nanoparticle surface area monitor (NSAM) (Fissan et al. 2007), miniDiSC (Fierz et al. 2011), Partector (Fierz et al. 2014) and Pegasor PPS-M (Rostedt et al. 2014; Järvinen et al. 2015). These instruments measure the total current of diffusion charged particles and convert it to the LDSA concentration using more or less a single conversion factor. This method is reasonably accurate up to the size about 300-600 nm, which enables for instance the measurement of combustion-generated particles in ambient environments (e.g. Kuula et al. 2019). However, it is reasonable to expect that, without any size dependency in measurements, the diffusion charger based measurement may underestimate the LDSA concentration if the studied aerosol contains particles larger than the aforementioned upper limit.

The outdoor LDSA concentrations that people are exposed to have been found to be at the highest close to traffic (Kuuluvainen et al. 2016), which is considered to be a significant risk to cause premature deaths by lung cancer (Raaschou-Nielsen et al. 2013). Particles from traffic emissions are mostly smaller than 200 nm (Pirjola et al. 2017). Thus, the aforementioned single conversion factor method for measuring the LDSA concentration is usually enough for a reasonably accurate LDSA measurement. However, high concentrations of particles up to 1 µm also exist in certain conditions in urban environments (Mönkkönen et al. 2005; Pirjola et al. 2017). Especially in the northern countries during the winter and spring the fraction of particles larger than 1 µm may increase significantly because

of the use of traction sand and studded tires (Johansson et al. 2007). This indicates that more accurate real-time measurement for LDSA with a wider measurement range is needed to have a better understanding of its sources and health effects in urban environment. Another major source of LDSA is residential wood combustion, where particle sizes are usually larger than in traffic (Pirjola et al. 2017), which contributes to higher surface area exposure with the same number of particles.

An electric low pressure impactor (ELPI) (Keskinen et al. 1992; Marjamäki et al. 2000) and its renewed version (ELPI+) (Järvinen et al. 2014) have been used to measure the LDSA concentration and size distribution by using the same single conversion factor method as the other common LDSA devices (Kuuluvainen et al. 2016; Kuuluvainen et al. 2018). This calibration however has the same inaccuracy with the suitable size range and in the size distribution measurement as discussed above. Thus, the method is insufficient for the LDSA size distribution measurements if the studied aerosol contains substantial amounts of particles larger than the aforementioned 300-600 nm.

In this study, the ELPI+ data analysis was developed to measure the LDSA concentration and size distribution by calculating stage-specific LDSA conversion factors for each of its fourteen impactor stages. The target is to achieve more accurate measurement of the LDSA size distribution and concentration in the measurement range from 6 nm to 10 µm. In addition, the conversion factors are calculated for the tracheobronchial and the head airways surface area deposition to achieve a comprehensive measurement of the total human respiratory tract surface area deposition. The analysis is compared to the single calibration factor method used e.g. for various LDSA sensors and e.g. by Kuuluvainen et al. (2016) for LDSA size distribution measurements (referred here as a single-factor method). In this paper, the particle surface area deposition in the alveolar region deposition is referred as LDSA and the other regions as tracheobronchial and head airways deposition.

ELPI+ Instrument

The electrical low pressure impactors, including the prototype (Keskinen et al., 1992) and the commercial versions (ELPI; Marjamäki et al., 2000, and ELPI+; Järvinen et al., 2014), all share a common operating principle. The ELPI takes the aerosol sample first into a unipolar diffusion charger. In the charger, unipolar corona discharge ionizes air and the unipolar charger ions are attached on the particles. The excess ions are removed from the flow by an electric field in an ion trap. The charged particles are then classified in a cascade impactor according to their aerodynamic size. Impactor stages are electrically insulated from each other and connected to electrometers. This enables the measurement of the particles by detecting the electric current, which is produced by the collected charged particles, from the separate stages. The electric current I that the collected charged particles produce after the charger is described with an equation

$$I = NPneQ, \tag{1}$$

where N is the particle number concentration, e the elementary charge, Q the flow rate through the instrument and Pn the charger efficiency function. The charger efficiency composes of particle penetration term P and average number of electric charges per particle after the charger n. The charger efficiency depends on particle mobility equivalent diameter, thus the particle effective density needs to be determined during the measurement. The charger efficiency has been previously determined in the ELPI+ calibration (Järvinen et al. 2014). The detection of the electric current in different impactor stages enables the measurement of particle number concentration in stages' size range, thus enabling the measurement of particle size distributions.

Measurement of the respiratory tract surface area deposition of particles by using ELPI+

Particle deposition in the human respiratory tract

The main mechanisms of particle deposition in the human respiratory tract are inertial impaction, sedimentation, interception and Brownian diffusion (Hoffman, 2011). As mentioned in the introduction, the deposition method and the region of deposition in the human respiratory tract depends on the particle size. The inertial impaction and sedimentation are the dominant deposition method for coarse particles larger than 1.0 µm, whereas the thermodynamic Brownian diffusion is dominant with particles smaller than 0.1 µm. A model for particle deposition in the human respiratory tract is presented in a report by International Commission on Radiological Protection (ICRP, 1994).

In the ICRP model, particle deposition in the different respiratory tract regions is determined semi-empirically by using parametrical values for inertial and Brownian deposition. In the model, the parametrical values for respiratory tract deposition depend e.g. on gender, age and breathing rate. Simplified equations for the respiratory tract deposition based on the ICRP model are represented for alveolar, tracheobronchial and head airways deposition in Hinds (1999). In these equations the deposition efficiency is calculated from the ICRP model by averaging male and female data with different physical activities i.e. breathing rates. These simplified equations are commonly used in the calculation of the respiratory tract deposition, since they give good information about the average particle exposure. These equations are used in this study as well.

In the Hinds' equations, particle deposition efficiency as a function of particle diameter is estimated for spherical particles with the unit density of 1 g/cm^3. Deposition curves for these equations are represented in Figure 1. The change of main deposition mechanism from the inertial effects to the Brownian diffusion can be seen as a drop in the deposition efficiencies near the size of 0.5 µm. Reason to this is that both inertial and Brownian depositions are relatively small in this size. The approximate efficiencies of inertial and Brownian

depositions are shown separately In Figure 2a.

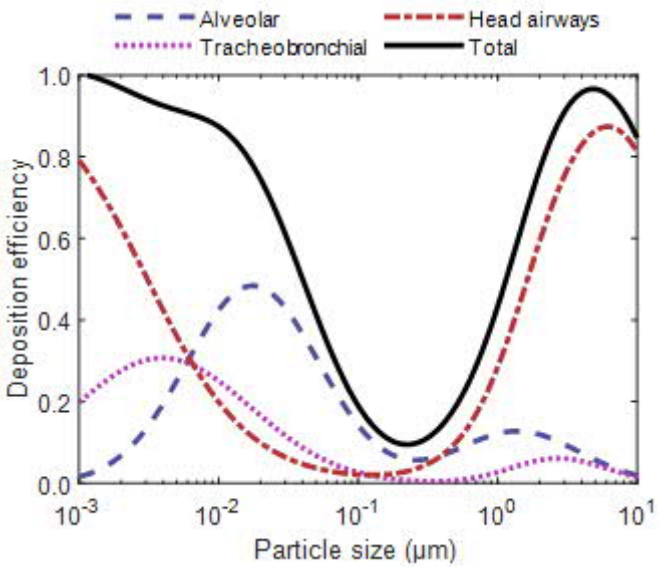

Figure 1. Particle deposition in the human respiratory tract as a function of particle size according to ICRP (1994) and Hinds (1999).

Change in particle density can change the inertial deposition efficiency, whereas it does not affect the Brownian deposition efficiency. The effect of the particle density in the deposition efficiencies as a function of particle mobility equivalent diameter is shown in Figure 2b. The change in particle density can be seen in the peak diameter of inertial deposition, which shifts to left or right depending on if density is higher or lower than the unit density, respectively. This effect needs to be taken into account in the deposition calculations. In Hinds (1999), it is suggested that, with particles larger than 0.5 µm, aerodynamic size should be used in the equation and, with particles smaller than 0.5 µm, mobility equivalent diameter should be used. This calculation causes deposition efficiency curves to be discontinuous in the size of 0.5 µm, due to the fact that the aerodynamic and mobility equivalent diameters are not equal. This discontinuity is shown in Figure 2b. It is also needed to determine, which diameter concept is used to determine the cut-off in the size of 0.5 µm. In reality, both inertial and Brownian deposition are acting simultaneously, which is significant in the size range from 0.1 µm to 1.0 µm. In the ICRP model, the total deposition efficiency is calculated by the equation

$$\mathrm{DF} = \sqrt{\mathrm{DF}_{\mathrm{inertial}}^2 + \mathrm{DF}_{\mathrm{Brownian}}^2}, \quad (2)$$

where $\mathrm{DF}_{\mathrm{inertial}}$ is the inertial deposition efficiency and $\mathrm{DF}_{\mathrm{Brownian}}$ the Brownian deposition efficiency. To take this into account with the simplified equations, two separate deposition functions for the inertial and the Brownian depositions needs to be determined. With this method, it is possible to estimate the change in the inertial deposition, which allows more accurate estimation for the particle deposition with different densities. In Hinds (1999) the alveolar deposition fraction as a function of particle size with the unit density is determined with the following equation

$$\mathrm{DF}_{\mathrm{al1}} = \left(\frac{0.0155}{d_p}\right)\left[\exp\left(-0.416(\ln d_{\mathrm{p}} + 2.84)^2\right) + 19.11\exp\left(-0.482(\ln d_{\mathrm{p}} - 1.362)^2\right)\right], \quad (3)$$

where d_p is the diameter (µm) of spherical particles with the unit density (1 g/cm^3). The equation is determined in two parts, which is also seen in the deposition curve in Figure 2a, which consists of two different peaks. The peak near the size of 20 nm can be approximated to represent the Brownian deposition, whereas the peak near 1.5 µm represents the inertial deposition.

By separating the function into two parts, deposition efficiencies for the Brownian and the inertial depositions can be written as

$$\mathrm{DF}_{\mathrm{al,Brownian}} = \left(\frac{0.0155}{d_{\mathrm{m}}}\right)\left[\exp(-0.416(\ln d_{\mathrm{m}} + 2.84)^2)\right], \quad (4)$$

$$\mathrm{DF}_{\mathrm{al,inertial}} = \left(\frac{0.0155}{d_{\mathrm{a}}}\right)\left[19.11\exp(-0.482(\ln d_{\mathrm{a}} - 1.362)^2)\right], \quad (5)$$

where d_m is the particle mobility equivalent diameter and d_a the aerodynamic diameter. Now, when the particle effective density is not the unit density, the change in the inertial deposition based on Equation 5, can be calculated as

$$\Delta\mathrm{DF}_{\mathrm{al,inertial}} = \mathrm{DF}_{\mathrm{al,inertial}}(d_{\mathrm{a}}) - \mathrm{DF}_{\mathrm{al,inertial}}(d_{\mathrm{m}}). \quad (6)$$

As mentioned above, the inertial deposition and the Brownian deposition occurs simultaneously, thus the change in the inertial deposition is not equal to the change in the total alveolar deposition. Now, Equation 2 is applied to estimate the effect of Equation 6 to the total deposition efficiency.

$$DF_{al} = DF_{al1} \pm \left(\sqrt{\Delta DF^2_{al,inertial} + DF^2_{al,Brownian}} - DF_{al,Brownian}\right). \qquad (7)$$

where the sign of the latter term depends on the sign of $\Delta DF_{al,inertial.}$ In all, this calculation method presented in Equations 3-7, is an approximation of the effect of the particle density in the human respiratory tract deposition, but as can be seen from Figure 2b, it gives more realistic result for the deposition curve than the discontinuous cut method in the size 0.5 µm, which Hinds (1999) suggests. Overall, the Hinds' equations are generalized and the actual deposition efficiencies of particles are individual and also depended on the person's physical activity. Thus, the deposition efficiencies in this study are based on the average case, which might differ slightly from the real exposure. However, the use of the average deposition efficiency gives useful information about the general particle exposure in different environments, which is important especially in monitoring measurements.

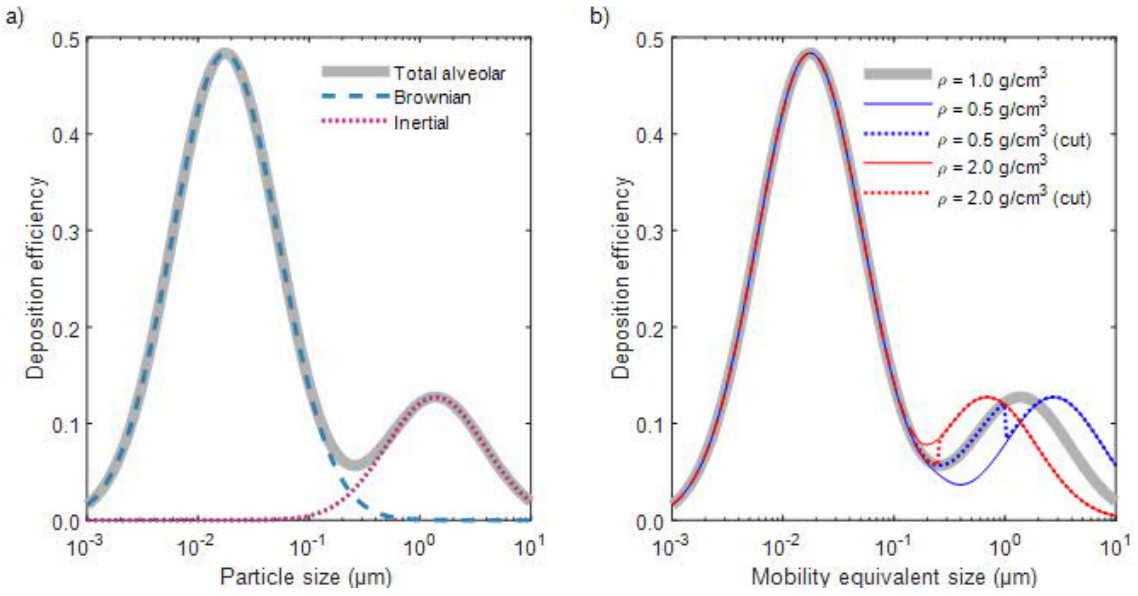

Figure 2. a) Particles' inertial, Brownian and the total deposition efficiency functions for alveolar region with the unit density of particles. b) Alveolar deposition efficiency

with different particle effective densities based on Equations 3-7. The efficiencies are also compared to the cut method, which was calculated by using aerodynamic particle size as the cut diameter in the size of 0.5 µm.

The same calculation method can also be applied for the tracheobronchial and the head airways deposition. The deposition efficiencies of these regions are shown in the Supplementary and the total deposition of particles in each region can be calculated by using Equation 7.

Conversion factors for ELPI+

In this study the conversion factors for ELPI+ are calculated for the alveolar, tracheobronchial and head airways surface area deposition. The conversion factors are calculated for the electric current data from the impactor stages, which is related to the aerosol concentration and size according to Equation 1. The calculation of the conversion factors is based on the general calibration of ELPI+ made by (Järvinen et al., 2014). The deposited surface area A_{dep} is determined simply by combining the particle number concentration N, particle surface area A and the total deposition efficiency in the region DF_{region}, which is estimated with Equation 7.

$$A_{\mathrm{dep}} = NA\mathrm{DF}_{\mathrm{region}}. \quad (8)$$

The ELPI+ response coefficient β is defined by dividing the deposited surface area concentration (Equation 8) with the electric current carried by the particles (Equation 1)

$$\beta = \frac{A_{dep}}{I} = \frac{\mathrm{ADF}_{region}}{PneQ}. \quad (9)$$

The particle effective density is required to be estimated in the ELPI+ measurement. This is because the ELPI+ classifies the particles according to their aerodynamic size and the charger efficiency depends on the particle mobility equivalent size. In the measurement of the respiratory tract deposition of particles, the effective density also affects the deposition efficiency of particles as mentioned

before. However, it needs to be noted that even though the particle effective density is estimated, the particle physical shape still affects the measurement accuracy, as the actual physical surface area of particles cannot be measured. The particles in this calculation are assumed to be spherical.

The LDSA response coefficients for ELPI+ with different effective densities of particles are shown in Figure 3. As can be seen, the response coefficient consists of two peaks and it increases rapidly with all shown densities near size 300 nm. This indicates that the single-factor method is not accurate for a LDSA measurement if the aerosol contains a significant particle concentration in sizes larger than 300 nm. The main reason for the increase is the fact that particle surface area is correlated with the square of the particle size, whereas the diffusion charged current correlates with the particle size nearly linearly. Particle effective density can also have significant impact to the response coefficient. With particles smaller than 300 nm, the effect of density can be seen mostly in the peak diameter, which shifts to right or left depending on density. This is because the cascade impactor classifies particles based on aerodynamic size, but in the human respiratory tract, the deposition of particles in this size range is dominated by the Brownian diffusion. Also, the particle charge after the charger depends on the mobility equivalent diameter (Equation 1). With larger particles, the effect can be seen in the height of the peak. This is because spherical particles with higher density have smaller physical size, thus they have smaller current than particles with lower density if their aerodynamic size is equal. Thus the response coefficient decreases as the density increases. ELPI+ charger efficiency function is a piecewise-defined function, which explains why the response coefficients shown in Figure 3 are not differentiable with certain particle sizes. The response coefficient for the tracheobronchial and the head airways deposition are shown in Supplementary.

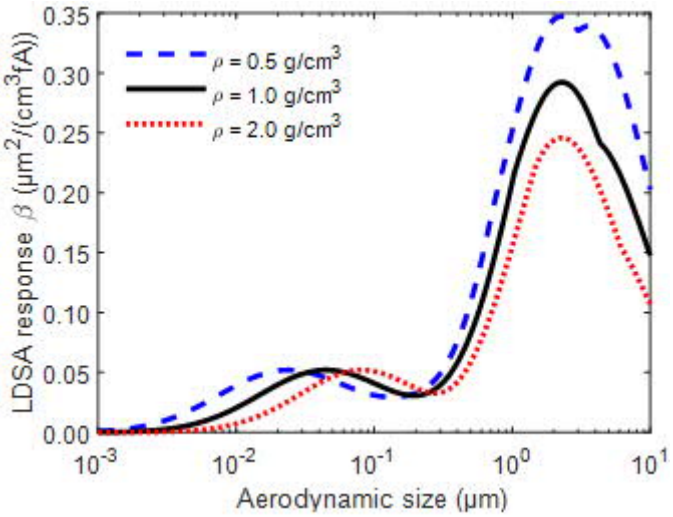

Figure 3. ELPI+ LDSA response coefficient β with different effective densities of particles.

To determine the conversion factor for each ELPI+ stage, cut-offs of the stages are needed to be analyzed. By approximating the stages' cut-offs to be ideal, the conversion factors can be determined by calculating the response coefficient factor β for the geometric mean of the stages' cut-off diameter. ELPI+ stage cut-offs are individual for each device, which means that the conversion factors are also slightly different for each device. However, the ELPI+ measurements with different instruments have shown to be well comparable with each other (Salo et al. 2019). The stages' geometric mean diameters for ELPI+, which is used in this study, are based on calibration made by Järvinen et al. 2014 and are shown in Table 1. Understandably, the ideal cut-off approximation causes small errors in the conversion factors, which is however acceptable due to the conceptual limitations of cascade impactor measurement as the resolution of impactor's size classification is limited. The conversion factors for the ELPI+ used in this study are calculated for spherical particles with the unit density and are shown in Table 1. According to Järvinen et al. 2014, the stages' cut-points have 2 % uncertainties with 95 % confidence intervals, thus the possible error in the stages' mean diameters is also 2 %. This uncertainty is shown in Table 1. As can be seen, the possible error is minimal even though it slightly increases with stages from 8 to 14. However, it needs to be noted that long-term measurements might affect the stages' collection efficiencies (Garra et al. 2016).

As mentioned, the estimation of particle effective density can be a source of inaccuracy in the measurement, and the density should be taken into account in the conversion factors. Conversion factors with different particle effective densities are shown in Supplementary to help selecting the correct conversion factors in different environments. If the particle density profile can be analyzed as a function of particle size, it is also possible to calculate the conversion factors for each stage separately with different density values. In Supplementary the conversion factor are also calculated with 10 % differences to the stages' geometrical mean diameters to help in the determination of conversion factors with different ELPI+ instruments.

Table 1. ELPI+ conversion factors to convert the electrical current data to particles' surface area concentrations deposited to alveolar (LDSA), tracheobronchial and head airways regions of human respiratory system. The factors have been calculated by using the unit density for spherical particles. The geometric mean diameter (dp_{mean}) of each ELPI+ impactor stage has been calculated based on instrument's calibration in Järvinen et al. (2014). Error bins are calculated from 2 % uncertainty of stages' cut-off diameters.

Stage (dp_{mean})	Alveolar ($\mu m^2/(cm^3 fA)$)	Tracheobronchial ($\mu m^2/(cm^3 fA)$)	Head airways ($\mu m^2/(cm^3 fA)$)
1 (9.71 nm)	0.0198 (0.0193-0.0203)	0.0120 (0.0119-0.0121)	0.0097 (0.0097-0.0097)
2 (21.8 nm)	0.0421 (0.0416-0.0426)	0.0137 (0.0137-0.0137)	0.0080 (0.0079-0.0080)
3 (40.6 nm)	0.0518 (0.0517-0.0519)	0.0123 (0.0122-0.124)	0.0066 (0.0066-0.0067)
4 (71.4 nm)	0.0478 (0.0474-0.0481)	0.0096 (0.0094-0.0097)	0.0059 (0.0059-0.0059)
5 (121 nm)	0.0368 (0.0364-0.0373)	0.0066 (0.0065-0.0067)	0.0067 (0.0066-0.0068)
6 (198 nm)	0.0307 (0.0307-0.0307)	0.0043 (0.0042-0.0043)	0.0125 (0.0121-0.0130)
7 (311 nm)	0.0410 (0.0400-0.0420)	0.0034 (0.0033-0.0034)	0.0321 (0.0306-0.0336)

8 (478 nm)	0.0765 (0.0741-0.0789)	0.0063 (0.0060-0.0067)	0.0893 (0.0851-0.0937)
9 (752 nm)	0.1486 (0.1447-0.1525)	0.0224 (0.0212-0.0237)	0.2613 (0.2495-0.2734)
10 (1.24 µm)	0.2440 (0.2411-0.2468)	0.0708 (0.0683-0.0733)	0.7157 (0.6919-0.7395)
11 (2.00 µm)	0.2898 (0.2890-0.2905)	0.1370 (0.01342-0.1396)	1.4371 (1.4013-1.4727)
12 (2.99 µm)	0.2824 (0.2809-0.2838)	0.1787 (0.1775-0.1798)	2.2202 (2.1790-2.2606)
13 (4.41 µm)	0.2405 (0.2395-0.2414)	0.1815 (0.1810-0.1819)	3.0533 (2.9857-3.1204)
14 (7.27 µm)	0.1927 (0.1953-0.1900)	0.1572 (0.1550-0.1594)	4.9353 (4.8544-5.0147)

The conversion factor for the single-factor method was also determined to estimate its accuracy. As can be seen in Figure 3, this is problematic, because one conversion factor cannot be generalized for the whole deposition range. Due to this, it is needed to choose, which size range is the most relevant in the measurement. In this study, the single conversion factor was determined for all deposition regions by calculating the response coefficient by using the particle size of 100 nm, which is commonly used in LDSA sensors (Fissan et al., 2007; Fierz et al., 2014). With the alveolar region, this is reasonable, because the response coefficient is fairly stable in the size range from 20 nm to 300 nm and, as mentioned, this size range is dominant in e.g. urban traffic environments (Kuuluvainen et al 2016). However, with the tracheobronchial and the head airways deposition, the response coefficient varies relatively notably more and the performance of the single-factor depends significantly on the dominant particle size. When the dominant particle size (reference particle size) was chosen to be 100 nm, the calculated single-factor coefficients for alveolar, tracheobronchial and head airways deposition were 0.041, 0.008 and 0.006 $um^2/(cm^3 fA)$ for ELPI+, respectively.

Experimental

Simulations

The stage-specific calibration of ELPI+ impactor was tested against various theoretical particle size distributions by simulating. First, the theoretical particle surface area deposition was calculated from number size distributions by using the deposition curves (Figure 1), which was then compared to ELPI+ simulation results. Simulated ELPI+ currents are based on the collection efficiency functions presented by (Järvinen et al. 2014). In the simulations, the particles were set to be spherical with the unit density (1 g/cm^3). Similar simulation was conducted for the single-factor method, and the results were compared to the theoretical values.

The simulations were carried out in two parts. First, narrow one-mode log-normal number size distributions with varying geometric mean diameters were simulated. Geometric standard deviation was set as 1.10 to achieve detailed dependence to the particle size. Additionally, simulations were also carried out with more realistic empirical distributions, which were based on experimental data obtained in urban environments reported by Mönkkönen et al. (2005) and Pirjola et al. (2017). Also, one distribution with coarse mode was included based on experimental data reported by Wu et al., (2009). These distributions are presented in Figure 4. The distribution A represents typical in traffic environments, where fresh nanoparticle emissions of traffic contribute to high concentration of particles smaller than 20 nm. The distribution C is more typical near combustion sources, such as residential wood combustion or biomass burning, and also in general during evenings and nights, when the aerosol can be more aged. The distribution B aims to describe a mixture of fresh and aged aerosol, which is also very typical in urban environments. The coarse mode in distribution D was measured in dust storm conditions in an urban environment, which can be comparable to the conditions during common street dust episodes.

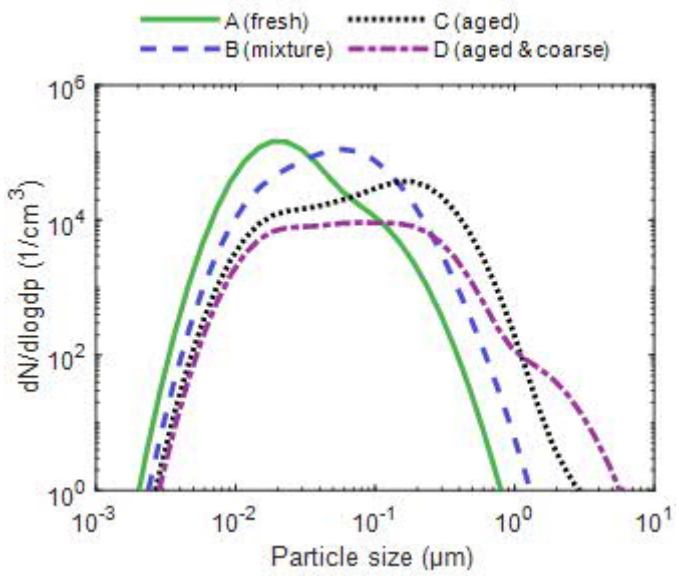

Figure 4: Empirical distributions used in the simulations. Distribution A represents typical in traffic environments (Pirjola et al., 2017), referred here fresh. Distribution C is typical near combustion sources, and also during evenings (Mönkkönen et al., 2005), referred here aged. Distribution B is a mixture of fresh and aged aerosol, which is also very typical in urban environments. The coarse mode in distribution D is measured in dust storm conditions (Wu et al., 2009), which can be compared to common street dust episodes.

Laboratory measurements

The calibration was also tested against real aerosol in laboratory measurements to support the simulation results. The laboratory measurements were carried out in two parts: with particles below 1 µm and then above 1 µm. For the smaller particles, an evaporation condensation generator (Liu and Lee, 1975) and a tubular furnace were utilized to generate liquid dioctyl sebacate particles (DOS, Alfa Aesar 95 %) and solid silicon dioxide (SiO2) particles, respectively. The SiO2 particles were produced by thermally decomposing tetraethyl orthosilicate (TEOS, Alfa Aesar 98%) in 1200 C. The generated particle size was controlled by adjusting the gas flow through the TEOS bubbler. Both DOS and SiO2 aerosols were diluted after the generation to achieve enough flow for the instrumentation.

The larger, over 1 µm, particles were generated with a rotating brush generator (Palas RBG 1000), which dispersed silicon carbide (SiC) test dust (Particle Technology Ltd., 0.5 to 10 µm). The produced aerosol was then directed into a residence time chamber to stabilize the particle concentration, along with a dilution flow, which was increased until the concentration was at a measurable level.

In addition to changing the produced particle materials, the used reference instrumentation changed between these two measurement ranges. For the smaller particles (< 1 µm), scanning mobility particle sizer (SMPS, TSI 3938) and condensation particle counter (CPC, TSI 3776) were used to determine the mobility number size distribution and the total number concentration. The reference for the bigger particles (> 1 µm) was aerodynamic particle sizer (APS, TSI 3321). In the measurements, the produced aerosol was monitored to be stable and each sample was measured for several minutes.

Results and discussion

Simulations

Results from the one-mode simulations for different deposition regions are shown in Figure 5. In the Figure, the total deposited surface area concentration calculated with both the stage-specific and the single-factor method are compared to the theoretical concentration. Results are shown for alveolar, tracheobronchial and head airways deposition, and also for total human respiratory system.

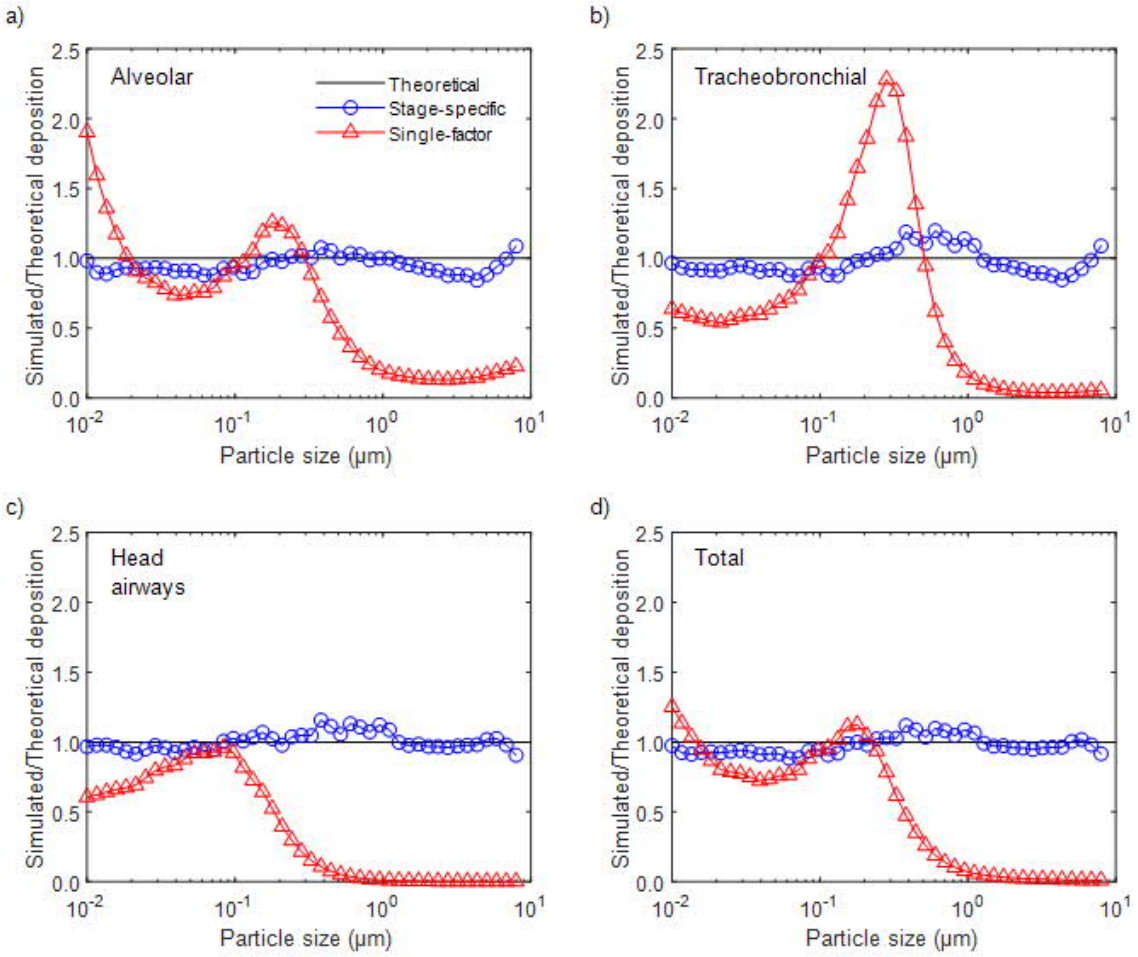

Figure 5: One-mode simulation results for a) alveolar (LDSA), b) tracheobronchial, c) head airways region and d) total respiratory tract deposition. The deposited surface area concentration with both stage-specific and single-factor method is compared to the theoretical concentration.

In the case of the alveolar region and the total respiratory tract deposition, the single-factor calibration correlates reasonably well in the size range from 20 nm to 300 nm. With all deposition regions, the accuracy of the single-factor method drops drastically if particles are larger than 300 nm. Also, in the measurement of the tracheobronchial and the head airways deposition particle surface area it is clearly incompetent. Instead, the stage-specific method correlates strongly with the theoretical deposition with all the deposition regions. The method is accurate in the whole simulated size range and the difference between the simulated and the theoretical result is less than 10 % with the majority of the simulated distributions. The result implies that the stage-specific method is accurate in the measurement of respiratory tract surface area deposition up to the size of 10

µm. With the stage-specific calibration, the minor differences between the theoretical values and the simulated values may come from the size classification, since the size resolution of cascade impactor measurement is limited, as mentioned in section 3.2.

Results regarding the empirical particle size distributions and their respiratory tract deposition are shown in Figure 6. The Figure shows the ratios of simulated and theoretical depositions, for particle size distributions A-D presented in Figure 4. Both the stage-specific and the single-factor method are reasonably accurate with the alveolar deposition with the distributions A and B, where the particles are mostly smaller than 300 nm. The accuracy of single-factor method can be explained with Figure 5 as the calibration errors can balance each other with wider distributions. As the mean particle size of the distributions increases, the accuracy of the single-factor method drops, whereas the stage-specific method gives accurate results. With the coarse mode distribution D, the error is significant. In Figure 7 the simulated LDSA size distributions are shown for distributions B and D. From the figure, it can be seen that the single-factor method is not capable to measure the coarse LDSA mode of distribution D, which explains the results in Figure 6. Also with the distribution B, some errors in the LDSA size distribution can be seen, as the mean diameter of the size distribution is overestimated. However, the results show that the single-factor method is good in the measurement of the total LDSA concentration, when the aerosol to be measured represents fresh exhaust or traffic site aerosol. The limitations of the single-factor method are clearer with the tracheobronchial and head airways depositions, where the results vary considerably with different distributions. Instead, the stage-specific method works well with these depositions also.

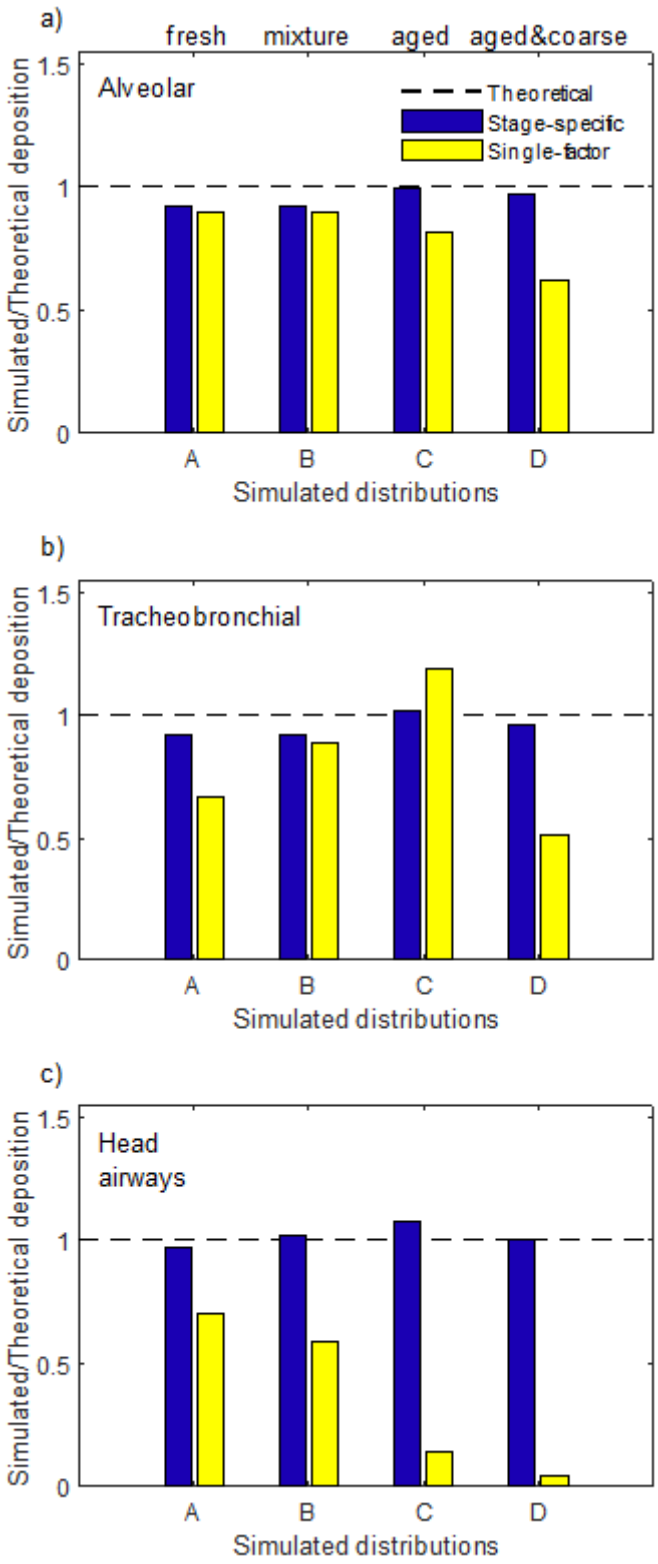

Figure 6. Ratio of simulated and theoretical particle surface area deposition in a) alveolar (LDSA), b) tracheobronchial, c) head airways region. Results are shown for all four particle size distributions presented in Figure 4.

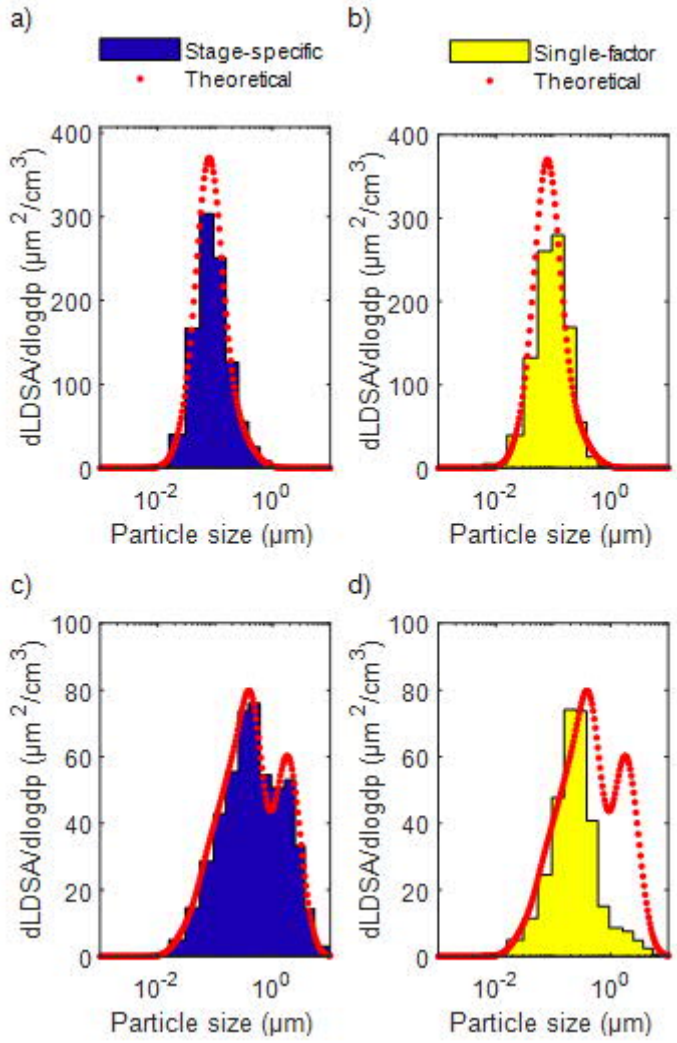

Figure 7. LDSA size distributions simulated with a) stage-specific, b) single-factor method from the empirical distribution B (mixture). c) Stage-specific and d) single-factor LDSA size distributions from the empirical distribution D (aged & coarse).

As mentioned in section 3.2, the particle effective density affects the LDSA measurement results. The sensitivity of results in respect of the determination of density was also analyzed with the empirical distributions. The sensitivity was analyzed by simulating the distributions A, B, C and D with certain particle densities varying from 0.3 g/cm^3 to 10.0 g/cm^3. Then the theoretical result was compared to results obtained by simulating the same particle size distribution with stage-specific method by using the unit density of particles. With the distributions A, B, C and D, the upper density limit corresponding to an error of 12 % compared to the theoretical result were roughly 9.9 g/cm^3, 4.8 g/cm^3, 1.4 g/cm^3

and 1.6 g/cm^3, respectively. With the distributions B, C and D, there was not lower density limit in the simulation range, but with the distribution A, the lower limit was roughly 0.8 g/cm^3. The result indicates that the accuracy of the stage-specific method is still reasonable even though the density is not carefully determined but known to be relatively close to the unit density. The effect to the LDSA size distribution can be analyzed by considering Figure 3. With particles smaller than 300 nm, the effect of change in particle density can be seen in the mean diameter of the LDSA size distribution. With particles larger than 300 nm, the effect can be seen in the measured total LDSA concentration. This can be seen in the simulations as well, as the distributions A and B are less sensitive to the effect of particle density in the total concentration than the distributions C and D because of the smaller fraction of particles larger than 300 nm. Again, with the single-factor method, the error in LDSA increases with the increase of share of particles larger than 300 nm. With the tracheobronchial and head airways deposition, the stage-specific method is more vulnerable to errors in the density estimation. The simulation results are shown in Supplementary.

Laboratory measurements

In the laboratory measurements, LDSA concentration measured with the stage-specific and with the single-factor calibration were compared to the reference measurement made with SMPS and APS. The reference LDSA was calculated from the measured number size distribution by using Equations 4-7. The calibration was tested against three different aerosols with mean particle size below 1 µm and against one aerosol with mean particle size 1 µm. The count mean diameter of the distributions, based on the reference measurement, were 55 nm, 115 nm, 200 nm (mobility equivalent diameter) and 2.0 µm (aerodynamic diameter) and the geometric standard deviation varied from 1.37 to 1.50. With the smaller particles, the particle effective density was determined by comparing the measured peak diameters of ELPI+ and SMPS. The measurement results of the LDSA concentration are shown in Figure 8.

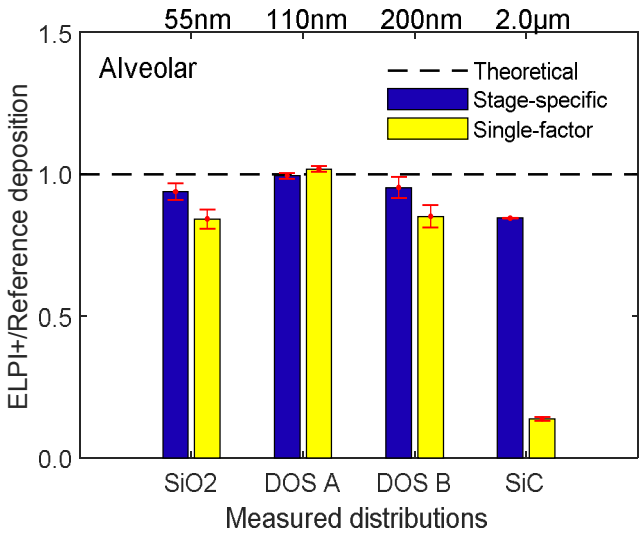

Figure 8. The LDSA concentration measured with the ELPI+ compared to the reference measurement conducted with SMPS (SiO2, DOS A, DOS B) and APS (SiC). The size values represent the count mean diameters of the distributions.

When analyzing the LDSA concentration of the SiO2 and DOS aerosols, both the stage-specific and the single-factor method applied for the ELPI+ data correlated relatively well with the reference measurement. However, the calibration errors of the single-factor method, shown in Figure 5a, can still be seen even though the errors are slightly balanced with each other with the wider size distributions. The single-factor method underestimates the LDSA in the size range from 20 nm to 100 nm, which explains the drop in the accuracy with the measured SiO2 aerosol. Again, with DOS B aerosol, the fraction of particles with the aerodynamic diameter larger than 300 nm is high, which contributes to the underestimation of LDSA measured with the single-factor method. The measured aerosol was stable, which reduced the error in the measurements.

In the case of the LDSA concentration of SiO2 and DOS aerosols, the average difference between the single-factor method and the SMPS reference was 10.7 %. For the stage-specific method this difference was 3.7 %, which indicates that the stage-specific method is notably more accurate in the measurement of the LDSA concentration than the single-factor method, even in the suitable particle size range of the single-factor measurement. When considering the coarse particle

measurement carried out with SiC particles, the single-factor method is clearly incompetent, whereas the stage-specific method gives again relatively good result. The slight drop in the accuracy of the stage-specific method with SiC particles can be explained with the drop in the response coefficient accuracy in the size range from 2 µm to 6 µm, shown in Figure 5a.

In Figure 9, the LDSA size distributions determined with both, the stage-specific and the single-factor method, are shown for the SiO2 and SiC – measurements. The underestimation of the single-factor method in the size range from 20 nm to 100 nm can be seen in the Figure 9, as the peak of the distribution is clearly underestimated, which explains the measurement error shown in Figure 8. With the SiC measurement the single-factor method clearly underestimates the whole LDSA size distribution. The results agree with the simulation results and they show that although the single-factor method gives a good estimation of the LDSA concentration with certain particle sizes, it is not as reliable method as the stage-specific ELPI+ calibration.

The measurement results of the tracheobronchial and the head airways depositions supports the simulation results as well and are shown in Supplementary. With the head airways region, it was noticed, that small errors in the ELPI+ diffusion correction can affect the results considerably, because with particles larger than 100 nm the response coefficient increases rapidly and the small errors in the stages' current can be significant in the measurement of surface area deposition. The same error can be seen in the measurement of the alveolar and the tracheobronchial surface area deposition, but it did not affect the results notably in this study. However, with larger particles, long-term measurements can affect the stages collection efficiencies, causing the upper stages collect more particles than they should (Garra et al. 2016). This can cause errors with alveolar and tracheobronchial regions as well.

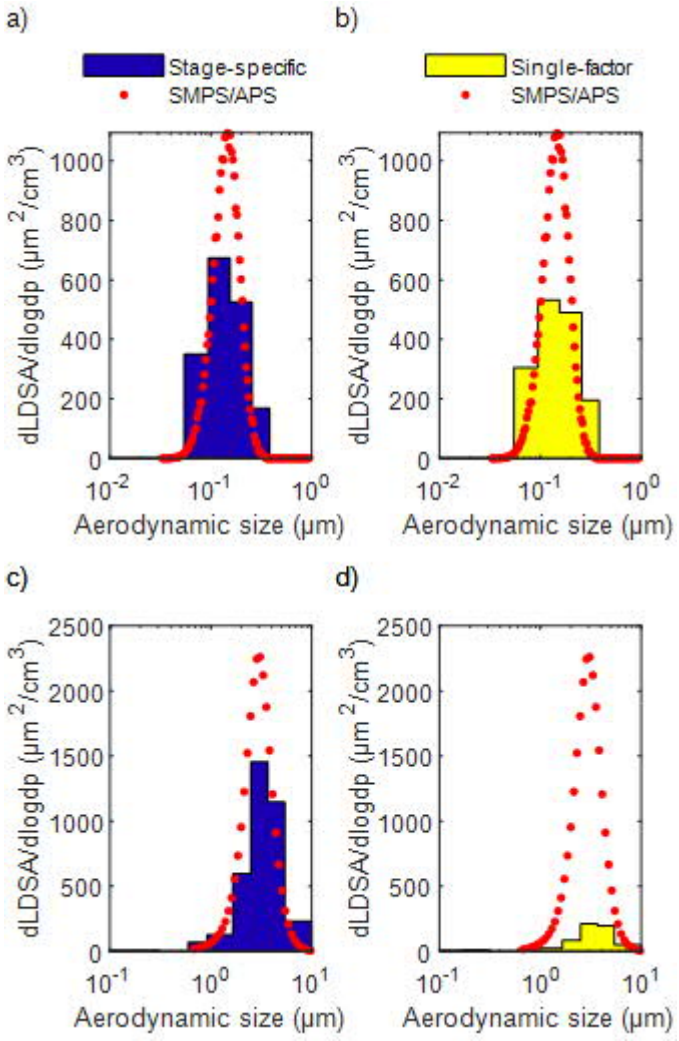

Figure 9. a) Stage-specific and b) single-factor LDSA size distributions of SiO2 (55 nm) –measurement, with SMPS as reference instrument. c) Stage-specific and d) single-factor LDSA size distributions of SiC (2.0 µm) measurement, with APS as reference instrument.

Conclusions

In all, the stage-specific calibration of ELPI+ showed good results against both simulations and laboratory measurements in the measurement of the deposited surface area of particles in the human respiratory tract. This was observed with large particle size range. With the alveolar region, the single-factor method, which is commonly used in various LDSA devices and also used e.g. by Kuuluvainen et al. (2016), gives reasonable results approximately up to the size of 300 nm, but with larger particles it can underestimate the LDSA concentration

significantly. Below the particle size of 300 nm, the stage-specific and the single-factor method are close to each other in the measurement of the LDSA concentration, but in the measurement of the LDSA size distribution, the stage-specific calibration is more reliable. With the tracheobronchial and the head airways surface area deposition, the stage-specific calibration performed well, whereas the single-factor method is clearly not suitable for these regions. Due to the higher conversion factors in the ELPI+ impactor stages from 9 to 14, it is important to calculate instrument's measurement losses and diffusion correction correctly, especially when measuring the head airways surface area deposition. It was found that errors in the stages' measured current can affect the results notably, if the stage's conversion factor differs considerably from the adjacent stages.

The conversion factors from electrical current data measured with ELPI+ to human respiratory tract deposited surface area concentrations, presented in this study, are based on the ELPI+ stages' collection efficiencies. This means that, in principle, the conversion factors need to be calculated separately for each ELPI+ instrument. However, the calculated conversion factors for the ELPI+ used in this study with different particle effective densities and 10 % differences in the stages' mean diameters are shown in Supplementary. Those can be used to evaluate the need for additional calibrations of individual instruments. The particle effective density affects the results and if the particle effective density profile is known as a function of particle size, it is possible to use more than one value of effective density in the calculation of conversion factors. The resolution of the stage-specific method could also be improved by applying inversion algorithms (Lemmetty et al., 2005; Saari et al., 2018) with the ELPI+ data.

The calculation in this study is based on the average model of the human respiratory tract deposition. In future studies, the calculation could be developed to include stage-specific conversion factors for different physical activities, gender and ages. This could be useful in monitoring measurements in different environments where certain groups of people or physical activities are more represented, and it could help in the analyzation of possible health effects of particles.

Acknowledgements:

The study was funded by Dekati Ltd.

References

Brown, D.M., Wilson, M.R., MacNee, W., Stone, V. & Donaldson, K. (2001). Size-Dependent Proinflammatory Effects of Ultrafine Polystyrene Particles: A Role for Surface Area and Oxidative Stress in the Enhanced Activity of Ultrafines, Toxicology and Applied Pharmacology, Vol. 175(3), pp. 191-199. https://www.sciencedirect.com/science/article/pii/S0041008X01992403.

Burnett RT, Pope CA III, Ezzati M, Olives C, Lim SS, Mehta S, Shin HH, Singh G, Hubbell B, Brauer M, Anderson HR, Smith KR, Balmes JR, Bruce NG, Kan H, Laden F, Prüss-Ustün A, Turner MC, Gapstur SM, Diver WR, Cohen A. 2014. An integrated risk function for estimating the global burden of disease attributable to ambient fine particulate matter exposure. Environ Health Perspect 122:397–403; http://dx.doi.org/10.1289/ehp.1307049

Dockery DW, Pope CA, xu X, Spengler JD, Ware JH, Fay ME, Ferris BG, Jr., Speizer FE. An association between air pollution and mortality in six U.S. cities. New Engl J Med 1993;329(24):1753-9.

Fierz, M., Meier, D., Steigmeier, P. & Burtscher, H. (2014). Aerosol Measurement by Induced Currents, Aerosol Science and Technology, Vol. 48(4), pp. 350-357. https://doi.org/10.1080/02786826.2013.875981

Fierz, M., Houle, C., Steigmeier, P. & Burtscher, H. (2011). Design, Calibration, and Field Performance of a Miniature Diffusion Size Classifier, Aerosol Science and Technology, Vol. 45(1), pp. 1-10. http://www.tandfonline.com/doi/abs/10.1080/02786826.2010.516283.

Fissan, H., Neumann, S., Trampe, A., Pui, D. & Shin, W. (2007). Rationale and principle of an instrument measuring lung deposited nanoparticle surface area, Journal of Nanoparticle Research, Vol. 9(1), pp. 53-59. DOI: 10.1007/978-1-4020-5859-2_6.

Garra, P., Trouve, G., Dieterlen, A., Kohler, S. (2016). Impactors long term collection errors and correction using reflected light microscopy. Journal of Aerosol Science. 91. 1-14. 10.1016/j.jaerosci.2015.09.006.

Hamilton, R. F., Jr, Thakur, S. A., & Holian, A. (2008). Silica binding and toxicity in alveolar macrophages. Free radical biology & medicine, 44(7), 1246–1258. doi:10.1016/j.freeradbiomed.2007.12.027

Hinds, W.C. (1999) Aerosol Technology, Properties, Behaviour, and Measurement of Airborne Particles. John Wiley & Sons Inc., New York.

Hofmann, W. (2011). Modelling inhaled particle deposition in the human lung—A review, Journal of Aerosol Science, Vol. 42(10), pp. 693-724. https://www.sciencedirect.com/science/article/pii/S0021850211000875.

ICRP, 1994. Human Respiratory Tract Model for Radiological Protection. ICRP Publication 66. Ann. ICRP 24 (1-3).

Johansson, C., Norman, M. & Gidhagen, L. Environ Monit Assess (2007) 127: 477. https://doi.org/10.1007/s10661-006-9296-4

Johnston, C.J., Finkelstein, J.N., Mercer, P., Corson, N., Gelein, R. & Oberdörster, G. (2000). Pulmonary Effects Induced by Ultrafine PTFE Particles, Toxicology and Applied Pharmacology, Vol. 168(3), pp. 208-215. https://www.sciencedirect.com/science/article/pii/S0041008X00990379.

Järvinen, A., Aitomaa, M., Rostedt, A., Keskinen, J. & Yli-Ojanperä, J. (2014). Calibration of the new electrical low pressure impactor (ELPI+), Journal of Aerosol Science, Vol. 69 pp. 150-159. https://www.sciencedirect.com/science/article/pii/S0021850213002528.

Järvinen, A., Kuuluvainen, H., Niemi, J.V., Saari, S., Dal Maso, M., Pirjola, L., Hillamo, R., Janka, K., Keskinen, J. and Rönkkö, T. (2015). Monitoring urban air quality with a diffusion charger based electrical particle sensor. Urban Clim. 14: 441–456.

Karlsson, H.L., Gustafsson, J., Cronholm, P. & Möller, L. (2009). Size-dependent toxicity of metal oxide particles—A comparison between nano- and micrometer size, Toxicology Letters, Vol. 188(2), pp. 112-118. https://www.sciencedirect.com/science/article/pii/S0378427409001611.

Keskinen, J., Pietarinen, K., Lehtimäki, M., 1992. Electrical low pressure impactor. J. Aerosol Sci. 23 (4), 353-360.

Kuuluvainen, H., Poikkimäki, M., Järvinen, A., Kuula, J., Irjala, M., Dal Maso, M., Keskinen, J., Timonen, H., Niemi, J.V. & Rönkkö, T. (2018). Vertical profiles of lung deposited surface area concentration of particulate matter measured with a drone in a street canyon, Environmental Pollution, Vol. 241 pp. 96-105. https://www.sciencedirect.com/science/article/pii/S0269749118301106.

Kuuluvainen, H., Rönkkö, T., Järvinen, A., Saari, S., Karjalainen, P., Lähde, T., Pirjola, L., Niemi, J.V., Hillamo, R. & Keskinen, J. (2016). Lung deposited surface area size distributions of particulate matter in different urban areas, Atmospheric Environment, Vol. 136 pp. 105-113. https://www.sciencedirect.com/science/article/pii/S1352231016303016.

Lelieveld, J., Evans, J. S., Fnais, M., Giannadaki, D., & Pozzer, A. (2015). The contribution of outdoor air pollution sources to premature mortality on a global scale. Nature, 525(7569), 367-371. doi:10.1038/nature15371

Lemmetty, M., Marjamäki, M., & Keskinen, J. (2005). The ELPI response and data reduction II: properties of kernels and data inversion. Aerosol Science and Technology, 39, 583–595.

Liu, B.Y.H., Lee, K.W. (1975) An aerosol generator of high stability, American Industrial Hygiene Association Journal, 36:12, 861-865, DOI: 10.1080/0002889758507357

Maher, B. A., Imad Ahmed, V. Karloukovski, D. A. MacLaren, P. G. Foulds, D. Allsop, D. M. A. Mann, R. Torres-Jardón, and L. Calderon-Garciduenas. 2016. “Magnetite Pollution Nanoparticles in the Human Brain.” Edited by Y. Rudich. Proceedings of the National Academy of Sciences 113 (39): 10797–801. https://www.pnas.org/content/113/39/10797.

Marjamäki, M., Keskinen, J., Chen, D. & Pui, D.Y.H. (2000). Performance evaluation of the electrical low pressure impactor (ELPI), Journal of Aerosol Science, Vol. 31(2), pp. 249-261. https://www.sciencedirect.com/science/article/pii/S002185029900052X.

Meister, K., Johansson, C. & Forsberg, B. (2012). Estimated Short-Term Effects of Coarse Particles on Daily Mortality in Stockholm, Sweden, Environmental health perspectives, Vol. 120(3), pp. 431-436. Available (accessed doi: 10.1289/ehp.1103995; 29): https://doi.org/10.1289/ehp.1103995.

Mönkkönen, P., Koponen, I.K., Lehtinen, K.E.J., Hämeri, K., Uma, R. & Kulmala, M. (2005). Measurements in a highly polluted Asian mega city: observations of aerosol number size distribution, modal parameters and nucleation events, Atmospheric Chemistry and Physics, Vol. 5(1), pp. 57-66. DOI: 10.5194/acpd-4-5407-2004

Oberdörster, G., Oberdörster, E., Oberdörster, J., 2005. Nanotoxicology: an emerging discipline evolving from studies of ultrafine particles. Environ. Health Perspect. 113 (7), 823-839.

Pirjola, L., J. V. Niemi, S. Saarikoski, M. Aurela, J. Enroth, S. Carbone, K. Saarnio, et al. 2017. Physical and chemical characterization of urban winter-time aerosols by mobile measurements in Helsinki, Finland.Atmos. Environ. 158:60–75.

Raaschou-Nielsen, O., Andersen, Z.J., Beelen, R.,Samoli, E., Stafoggia, M., Weinmayr, G.,Hoffmann, B., Fischer, P., Nieuwenhuijsen, M.J., Brunekreef, B., et al., 2013. Air pollution and lung cancer incidence in 17 European cohorts: prospective analyses from the European study of cohorts for air pollution effects (ESCAPE). LancetOncol. 14, 813–822

Rostedt, A., Arffman, A., Janka, K., Yli-Ojanperä, J. and Keskinen, J. (2014). Characterization and response model of the PPS-M aerosol sensor. Aerosol Sci. Technol. 48: 1022–1030.

Salo, L., Mylläri, F., Maasikmets, M., Niemelä, V., Konist, A., Vainumäe, K., Kupri, H, Titova, R., Simonen, P., Aurela, M., Bloss, M., Keskinen, J., Timonen, H., & Rönkkö, T. (2019): Emission measurements with gravimetric impactors and electrical devices: An aerosol instrument comparison, Aerosol Science and Technology, DOI: 10.1080/02786826.2019.1578858

Wu, Z. J., Cheng, Y. F., Hu, M., Wehner, B., Sugimoto, N., and Wiedensohler, A.: Dust events in Beijing, China (2004–2006): comparison of ground-based measurements with columnar integrated observations, Atmos. Chem. Phys., 9, 6915-6932, https://doi.org/10.5194/acp-9-6915-2009, 2009.